Proceedings of the Project Review, Geo-Mathematical Imaging Group (Purdue University, West Lafayette IN), Vol. 1 (2012) pp. 305-318.

ON TIME-HARMONIC SEISMIC DATA AND BLENDING IN FULL WAVEFORM INVERSION

SUNYOUNG PARK*, LINGYUN QIU†, MAARTEN V. DE HOOP‡, AND CHANGSOO SHIN§

Abstract. In this paper, we study the relationship between the acquisition of time-harmonic seismic data and the Dirichlet-to-Neumann map for the Helmholtz equation in dimension $n \geq 3$. This relationship is established through the introduction of a single-layer potential operator. We analyze its properties with a view to so-called iterative full waveform inversion based on the Hilbert-Schmidt norm, that is, its (conditional) convergence on the one hand and a sparse, spectral source blending approach with controlled error on the other hand.

1. Introduction. In this paper, we study the relationship between the acquisition of time-harmonic seismic data and the Dirichlet-to-Neumann map in dimension $n \geq 3$. This relationship is established through the introduction of a single-layer potential operator. This single-layer potential operator is directly related to what seismologists refer to as source blending. We analyze its properties with a view to so-called full waveform inversion based on the Hilbert-Schmidt norm. In the process, we also review the equivalent data types.

The properties we are interested in, concern the difference of two single-layer potential operators evaluated in distinct wave speed models while the configuration is the same. We address (i) the stability of the inverse problem using the single-layer potential operator as the data. To this end, we relate this stability to the corresponding stability using the Dirichlet-to-Neumann map as the data. The latter stability is conditionally Lipschitz, see Beretta, De Hoop and Qiu [3], which is the counterpart of a similar result in electrical impedance tomography (EIT), see Alessandrini and Vesella [1]. Moreover, we (ii) estimate the singular spectrum of the mentioned difference of operators. We carry out this estimate in the case that the two wave speed models coincide and are smooth in a small neighborhood of the acquisition surface. This is relevant in full waveform inversion when the wave speed model is known in the vicinity of the source and receiver arrays, for example, in marine acquisition. The relationship between the single-layer potential operator and the Dirichlet-to-Neumann map can be found in Nachman [18].

The (conditional) stability property provides a convergence criterion for full waveform inversion (De Hoop, Qiu and Scherzer [12]). The estimate for the singular spectrum of the difference of two single-layer potential operators, specifically the rapid decay of the singular values, justifies the introduction of a Schatten norm for the objective functional. In fact, the mentioned difference of single-layer potential operators is a trace-class operator. With the estimated decay, we truncate the singular spectrum and then use the corresponding singular functions in the blending process. The number of significant singular values is relatively small, and hence, relatively few experiments are needed for the full waveform inversion to be effective.

The process of source blending has appeared in various acquisition and imaging strategies. Perhaps the most basic form involves synthesizing source plane waves from point source data in plane-wave migration [25]. So-called controlled illumination [21]) can also be viewed as a particular blending strategy. In blended acquisition, typically, time-overlapping shot records are generated in the field by using incoherent source arrays; for simultaneous source firing see Beasley, Chambers and Jiang [2] and for near simultaneous source firing see Stefani, Hampson and Herkenhoff [22]. Berkhout, Blacquire and Verschuur [6, 5] considered simple time delays for the blending process, allowing the use of conventional sources in acquisition. The use of simultaneous random sources have been proposed, further, by [20] and others.

The use of simultaneous sources in linearized inverse scattering was studied by Dai and Schuster [11], and in full waveform inversion, for example, by Vigh and Starr [23] (synthesizing source plane

*Department of Energy Resources Engineering, Seoul National University, Seoul, Korea.
†Department of Mathematics, Purdue University, West Lafayette, IN 47907, USA.
‡Department of Mathematics, Purdue University, West Lafayette, IN 47907, USA (mdehoop@purdue.edu).
§Department of Energy Resources Engineering, Seoul National University, Seoul, Korea.

waves), Krebs *el al.* [17] (random source encoding) and Gao, Atle and Williamson [13] (deterministic source encoding). In global tomography, source "stacking" was introduced by Capdeville, Gung and Romanowicz [8].

For general references to the nonlinear inverse problems for the Helmholtz equations and layer potentials, see Colton & Kress [10] and Isakov [16].

Our functional in the optimization is expressed in terms of the operator norm of the single-layer potential operator. In general, however, the estimation of this norm is a significant computational effort. Hence, to improve efficiency, we relate the operator norm of the residual (the difference of two single-layer potential operators) to the Schatten p-norm, and, in practice, to the Hilbert-Schmidt norm (that is, $p = 2$). These norms are expressed in terms of the singular spectrum of the residual operator, and, then, we truncate the spectrum exploiting its rapid decay. The singular functions corresponding with these significant singular values then represent important blending functions mentioned above. This idea is motivated by the work of Gisser, Isaacson and Newell [15] in EIT, who designed an approach to construct a current density which gives optimal resolution of the nonlinear inverse conductivity problem. As an alternative approach, using a set of prescribed currents, we mention the variationally constrained iterative reconstruction method for EIT developed by Borcea, Gray and Zhang [7].

In the full waveform inversion, considered here, multiple scattered waves are naturally accounted for. We point out that the kernels of the single-layer potential operator and of its inverse, which play a role in our study, were, essentially, used by Berkhout [4] in his method to remove multiple scattering from the boundary.

The outline of the paper is as follows. In the next section, we discuss the modelling of seismic reflection data and introduce the single-layer potential operator. We establish the boundedness of this operator and its inverse. In Section 3, we introduce the Dirichlet-to-Neumann map, also in terms of the Dirichlet eigenfunctions (normal modes) of the Helmholtz operator. We discuss its relation with the single-layer potential operator. We then show that (conditional) stability of the inverse problem with the single-layer potential operator as the data follows from the (conditional) stability with the Dirichlet-to-Neumann map as the data. In Section 4, we estimate the decay of the singular values of the difference of two single-layer potential operators under certain conditions of the underlying wave speed models. We then introduce the Schatten norm and an optimization strategy based on singular functions. In Section 5, we show a numerical example illustrating the decay of the mentioned singular spectrum using a direct structured Helmholtz solver [24].

2. Modelling the data: The single-layer potential operator. We consider time-harmonic waves, described by solutions, u say, of the Helmholtz equation on a bounded open domain $\Omega \subset \mathbb{R}^n$. The boundary, $\partial\Omega$ is in $C^{(1,1)}$, and $\Omega' = \mathbb{R}^n \backslash \bar{\Omega}$ is connected. We write

$$\tilde{q}(x) = -\omega^2 c^{-2}(x),$$

and keep $\omega \in \mathbb{R}$ fixed; we assume that $c^{-2} \in L^\infty(\Omega)$. We have the general formulation

$$\begin{cases} (-\Delta + \tilde{q}(x))u &= f, \quad x \in \Omega, \\ u &= g, \quad x \in \partial\Omega. \end{cases} \tag{2.1}$$

Here, f represents sources, and g boundary values.

We mention the existence and uniqueness of solutions in (see Gilbarg & Trudinger [14])

PROPOSITION 2.1. *Assume that* 0 *is not a Dirichlet eigenvalue for* $-\Delta + \tilde{q}$ *in* Ω, $\tilde{q}$ *is a function in* $L^\infty(\Omega)$, $f \in L^p(\Omega)$ *and* $g \in W^{2-1/p,p}(\partial\Omega)$, $1 < p < \infty$. *Then there is a unique solution* $u \in W^{2,p}(\Omega)$ *of (2.1). Moreover*

$$\|u\|_{W^{2,p}(\Omega)} \leq C\left(\|g\|_{W^{2-1/p,p}(\partial\Omega)} + \|f\|_{L^p(\Omega)}\right), \tag{2.2}$$

where C *depends only on* p, Ω *and* $\|\tilde{q}\|_{L^\infty(\Omega)}$.

We apply this theorem for $p = 2$, assuming sufficient regularity for f and g. (We note that $W^{2,2}$, $W^{3/2,2}$, coincide with H^2, $H^{3/2}$, respectively.) Seismic reflection data are generated by point sources on $\partial\Omega$ and observed at points on $\partial\Omega$. In preparation of a description of the data in terms of fundamental solutions in $\mathbb{R}^n$, we extend $\tilde{q}(x)$ to a function with value

$$-k^2 = -\omega^2 c_0^{-2} \tag{2.3}$$

in Ω'. Let $G_k^+(x, y)$ be the outgoing Green's function for the Helmholtz equation with constant coefficient, c_0^{-2}, in $\mathbb{R}^n$, which is given by

$$\begin{aligned} G_k^+(x,y) &= \frac{1}{(2\pi)^n} \int \frac{e^{\mathrm{i}(x-y)\xi}}{\xi^2 - k^2 - \mathrm{i}0} \mathrm{d}\xi \\ &= \frac{\mathrm{i}}{4} \left(\frac{|k|}{2\pi |x-y|} \right)^{(n-2)/2} H^{(1)}_{(n-2)/2}(|k||x-y|). \end{aligned} \tag{2.4}$$

We set

$$q(x) = \tilde{q}(x) + k^2,$$

which is compactly supported. We assume that k^2 is not an eigenvalue of $-\Delta + q$ on Ω. We let $\mathcal{G}_{q,k}(x, y)$ be the solution of

$$(-\Delta_x + q - k^2)\, \mathcal{G}_{q,k}(x,y) = \delta(x-y), \quad x, y \in \mathbb{R}^n, \tag{2.5}$$

satisfying the Sommerfeld radiation condition as $|x| \to \infty$. Restricting x and y to $\partial\Omega$ yields the seismic reflection, or Cauchy, data:

$$\mathcal{A} = \{\mathcal{G}_{q^\dagger,k}(x,y) \mid \ x, y \in \partial\Omega,\ x \neq y\},$$

if $q^\dagger(x)$ signifies the "true" model.

In the constant "background" model with wave speed c_0, we introduce the operator,

$$S_k^+ :\ H^{1/2}(\partial\Omega) \to H^{3/2}(\partial\Omega),$$

by

$$S_k^+ w(x) = \int_{\partial\Omega} G_k^+(x,y)\, w(y)\, \mathrm{d}\sigma(y), \quad x \in \partial\Omega, \tag{2.6}$$

which is bounded. Here, $\mathrm{d}\sigma$ is the natural area element on $\partial\Omega$. In a general heterogeneous model, we introduce

$$\mathcal{S}_{q,k} :\ H^{1/2}(\partial\Omega) \to H^{3/2}(\partial\Omega),$$

with

$$\mathcal{S}_{q,k} w(x) = \int_{\partial\Omega} \mathcal{G}_{q,k}(x,y)\, w(y)\, \mathrm{d}\sigma(y), \quad x \in \partial\Omega, \tag{2.7}$$

which is bounded also [18, Theorem 1.6]. The (source) blended data are then represented by

$$\mathcal{B} = \{\mathcal{S}_{q^\dagger,k} w \mid \ w \in H^{1/2}(\partial\Omega)\}.$$

PROPOSITION 2.2. *Assume that k^2 is not a Dirichlet eigenvalue of $-\Delta + q$ or of $-\Delta$ in Ω. Then the inverse, $(S_k^+)^{-1}$, of operator S_k^+ exists and is bounded, $H^{3/2}(\partial\Omega) \to H^{1/2}(\partial\Omega)$. Moreover, the inverse, $\mathcal{S}_{q,k}^{-1}$, of operator $\mathcal{S}_{q,k}$ exists and is bounded, $H^{3/2}(\partial\Omega) \to H^{1/2}(\partial\Omega)$.*

For a proof of this Proposition, see [18, Section 6]. Essentially, it follows that

$$\mathcal{S}_{q,k} = S_k^+[I + (S_k^+)^{-1}(\mathcal{S}_{q,k} - S_k^+)]$$

is invertible by showing that -1 cannot be an eigenvalue of $(S_k^+)^{-1}(\mathcal{S}_{q,k} - S_k^+)$. It is possible to express $\mathcal{S}_{q,k}^{-1}$ in terms of the difference of an interior and an exterior Dirichlet-to-Neumann map, which are both bounded.

3. Stability analysis.

3.1. Dirichlet-to-Neumann map. A well-known approach for inverse scattering problems is to enclose all inhomogeneities in an artificial bounded domain Ω. Then one imposes a boundary condition on the boundary $\partial\Omega$, which gives the same solution in Ω as in the original problem of the larger domain. One considers the Dirichlet-to-Neumann map as the data. We will re-express these data in terms of the single-layer potential operator.

To capture realistic acquisition geometries, we may consider partial boundary data. That is, we generate data on Σ, an open portion of $\partial\Omega$.

DEFINITION 3.1. *Let Σ be a open portion of $\partial\Omega$. We define $H^{1/2}_{co}(\Sigma)$ as*

$$H^{1/2}_{co}(\Sigma) = \{g \in H^{1/2}(\partial\Omega) \mid \operatorname{supp} g \subset \Sigma\}$$

and $H^{-1/2}_{co}(\Sigma)$ as the topological dual of $H^{1/2}_{co}(\Sigma)$; we denote by $\langle\cdot,\cdot\rangle$ the dual pairing between $H^{1/2}_{co}(\Sigma)$ and $H^{-1/2}_{co}(\Sigma)$.

DEFINITION 3.2. *Let Σ be a open portion of $\partial\Omega$ and q be a real-valued function in L^∞. Assume that 0 is not a Dirichlet eigenvalue of $(-\Delta+\tilde{q})$ in Ω. For any $g \in H^{1/2}_{co}(\Sigma)$, let $u \in H^1(\Omega)$ be the weak solution to the Dirichlet problem*

$$\left\{\begin{array}{rcll} (-\Delta+\tilde{q}(x))u &=& 0, & x\in\Omega, \\ u &=& g, & x\in\partial\Omega. \end{array}\right. \tag{3.1}$$

We define the local Dirichlet-to-Neumann map $\Lambda^{(\Sigma)}_q$ as

$$\begin{array}{rrl} \Lambda^{(\Sigma)}_{\tilde{q}}: & H^{1/2}_{co}(\Sigma) \to & H^{-1/2}_{co}(\Sigma) \\ & g \mapsto & \left.\dfrac{\partial u}{\partial \nu}\right|_{\Sigma}, \end{array}$$

where ν is the exterior unit normal vector to $\partial\Omega$.

The Dirichlet-to-Neumann map is analytic in frequency. We note that $\Lambda^{(\Sigma)}_{\tilde{q}}$ is contained in the Banach space $\mathcal{L}(H^{1/2}_{co}(\Sigma), H^{-1/2}_{co}(\Sigma))$; we will take $\Sigma = \partial\Omega$ from now on. This follows from the fact that $\Lambda_{\tilde{q}}$ is bounded $H^{3/2}(\partial\Omega) \to H^{1/2}(\partial\Omega)$ and that $H^{-1/2}(\partial\Omega)$ is dense in $H^{-1/2}(\partial\Omega)$ through an extension of $\Lambda_{\tilde{q}}$.

Normal modes of the Helmholtz operator. Here, we summarize the representation of the Dirichlet-to-Neumann map in terms of eigenfunctions of the Helmholtz operator; see [19, 9]. We set $\lambda = k^2$ and consider the Dirichlet boundary problem in (3.1):

$$\left\{\begin{array}{rcll} (-\Delta+q-\lambda)u &=& 0, & x\in\Omega, \\ u &=& g, & x\in\partial\Omega. \end{array}\right. \tag{3.2}$$

The eigenfunctions with Dirichlet boundary condition are denoted by $\phi_j(q)$, $j = 1, 2, \dots$ corresponding with eigenvalues $\lambda_j(q)$.

The Dirichlet-to-Neumann map, $\Lambda_{q-\lambda}$, can be represented with spectral data:

$$\Lambda_{q-\lambda} g \text{ “ = ” } \sum_{j=1}^{\infty} \frac{1}{\lambda-\lambda_j(q)} \frac{\partial\phi_j(q)}{\partial\nu} \left(g, \frac{\partial\phi_j(q)}{\partial\nu}\right)_{L^2(\partial\Omega)}. \tag{3.3}$$

Since the series on the right-hand side does not absolutely converge in some cases, one uses **[ref]** some high order derivative of the Dirichlet-to-Neumann map,

$$\Lambda^{(m)}_{q-\lambda} := \frac{d^m}{d\lambda^m}\Lambda_{q-\lambda}. \tag{3.4}$$

The series for this map converges absolutely for $m \gg 1$, because $\lambda_j(q)^{-m-1} \sim j^{-2(m+1)/n}$ decays rapidly for $m \gg 1$. If $m > n/2 + 3/4$, then

$$\Lambda^{(m)} g = -m! \sum_{j \geq 1} \frac{1}{(\lambda_j(q) - \lambda)^{m+1}} \left(\int_{\partial\Omega} g \, \frac{\partial \phi_j(q)}{\partial \nu} \mathrm{d}\sigma \right) \frac{\partial \phi_j(q)}{\partial \nu} \tag{3.5}$$

converges absolutely in $H^{1/2}(\partial\Omega)$. From this, we obtain

$$\begin{aligned} \Lambda_{q-\lambda} g = \int_{-\infty}^{\lambda} \mathrm{d}\lambda_1 \int_{-\infty}^{\lambda_2} \mathrm{d}\lambda_2 \cdots \int_{-\infty}^{\lambda_{m-1}} \mathrm{d}\lambda_m& \\ (-m!) \sum_{j \geq 1} \frac{1}{(\lambda_j(q) - \lambda_m)^{m+1}} \left(\int_{\partial\Omega} g \, \frac{\partial \phi_j(q)}{\partial \nu} \mathrm{d}\sigma \right) \frac{\partial \phi_j(q)}{\partial \nu}&. \end{aligned} \tag{3.6}$$

3.2. From single-layer potential operator to Dirichlet-to-Neumann map. From S_k^+, we can build the relation between $\mathcal{S}_{q,k}$ and the Dirichlet-to-Neumann map. We have

$$\Lambda_{q-k^2} = \Lambda_{-k^2} + \mathcal{S}_{q,k}^{-1} - (S_k^+)^{-1}, \tag{3.7}$$

or

$$\mathcal{S}_{q,k} - S_k^+ = -S_k^+ \left(\Lambda_{q-k^2} - \Lambda_{-k^2} \right) \mathcal{S}_{q,k}. \tag{3.8}$$

This identity is defined on $H^{1/2}(\partial\Omega)$, and can be derived from the resolvent equation,

$$\mathcal{G}_{q,k}(x,y) = G_k^+(x-y) - \int_{\Omega} G_k^+(x-z) q(z) \mathcal{G}_{q,k}(z,y) \, \mathrm{d}z. \tag{3.9}$$

For $w \in H^{1/2}(\partial\Omega)$, we the find that

$$\mathcal{S}_{q,k} w(x) - S_k^+ w(x) = - \int_{\Omega} G_k^+(x-z) q(z) (\mathcal{S}_{q,k} w)(z) \, \mathrm{d}z. \tag{3.10}$$

From (3.7) we straightforwardedly obtain

$$\Lambda_{q-k^2} - \Lambda_{q^\dagger - k^2} = \mathcal{S}_{q,k}^{-1} - \mathcal{S}_{q^\dagger,k}^{-1}, \tag{3.11}$$

or

$$\Lambda_{q-k^2} - \Lambda_{q^\dagger - k^2} = -\mathcal{S}_{q^\dagger,k}^{-1} (\mathcal{S}_{q,k} - \mathcal{S}_{q^\dagger,k}) \mathcal{S}_{q,k}^{-1}$$

It is immediate that

$$\|\mathcal{S}_{q,k} - \mathcal{S}_{q^\dagger,k}\| \leq \|\mathcal{S}_{q,k}\| \, \|\mathcal{S}_{q^\dagger,k}\| \, \|\Lambda_{q-k^2} - \Lambda_{q^\dagger - k^2}\|,$$

but using Proposition 2.2, it also follows that

$$\|\Lambda_{q-k^2} - \Lambda_{q^\dagger - k^2}\| \leq \|\mathcal{S}_{q,k}^{-1}\| \, \|\mathcal{S}_{q^\dagger,k}^{-1}\| \, \|\mathcal{S}_{q,k} - \mathcal{S}_{q^\dagger,k}\|. \tag{3.12}$$

As a consequence, (conditional) Lipschitz stability for the Dirichlet-to-Neumann map implies (conditional) Lipschitz stability for the single-layer potential operator:

$$\|q - q^\dagger\|_{L^\infty(\Omega)} \leq C \, \|\mathcal{S}_{q,k} - \mathcal{S}_{q^\dagger,k}\|.$$

Here, C depends on parameters determining the class of functions guaranteeing the Lipschitz stability.

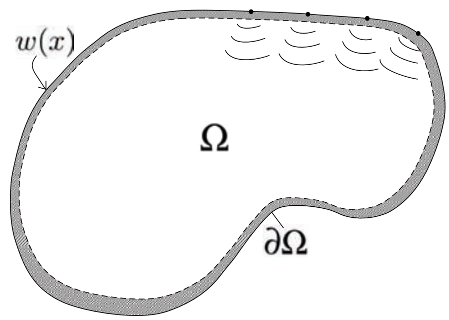

FIG. 1. *The domain Ω and point sources on its boundary. The models, q and $q^\dagger$, are smooth and coincide in the grey boundary layer. The blending described by w is applied in the boundary.*

4. Objective functional for full waveform inversion. We consider the nonlinear operator,

$$F: \ L^\infty \to \mathcal{L}(H^{1/2}, H^{3/2}), \quad q \to \mathcal{S}_{q,k}$$

and the functional

$$\mathcal{J}(q) = \tfrac{1}{p}\|F(q) - F(q^\dagger)\|^p = \tfrac{1}{p}\|\mathcal{S}_{q,k} - \mathcal{S}_{q^\dagger,k}\|^p,$$

with the usual definition,

$$\|\mathcal{S}_{q,k} - \mathcal{S}_{q^\dagger,k}\| = \sup_{w\in H^{1/2}(\partial\Omega),\ \|w\|=1} \|(S_{q,k} - \mathcal{S}_{q^\dagger,k})(w)\|_{H^{3/2}(\Omega)}.$$

Using the conditional stability, as in De Hoop, Qiu and Scherzer [12], we can generate a convergent Landweber iteration to recover $q^\dagger$ starting from an admissible initial choice of q.

Here, we introduce a different operator norm for the difference, $\mathcal{S}_{q,k} - \mathcal{S}_{q^\dagger,k}$, namely in terms of its singular spectrum. We assume that q, $q^\dagger$ are smooth at and near the boundary, $\partial\Omega$. Moreover, we assume that q and $q^\dagger$ coincide at and near the boundary. We illustrate the configuration in Figure 1.

The kernel of $\mathcal{S}_{q,k} - \mathcal{S}_{q^\dagger,k}$ is the difference of Green's functions with "end" points on the boundary. The difference of the Green's functions solves

$$(-\Delta_x + q(x) - k^2)(\mathcal{G}_{q,k} - \mathcal{G}_{q^\dagger,k})(x, y) = 0,$$

for points x near the boundary, where q is either of the potentials (they are equal there). Then $\mathcal{G}_{q,k} - \mathcal{G}_{q^\dagger,k}$ is smooth in x by elliptic regularity with values distributions in the y variable. We can even say that $\mathcal{G}_{q,k} - \mathcal{G}_{q^\dagger,k}$ is smooth in (x, y) since it is in the kernel of the elliptic operator $\Delta_x + \Delta_y + q(x) + q(y) - 2k^2$. It follows that the difference operator is smoothing. Hence, its singular values will decay rapidly. We note that the difference operator is a Hilbert-Schmidt operator. Moreover, it now follows that this operator is a trace-class operator.

Given the decay of the singular spectrum, we can take as the operator norm the Schatten p-norm:

$$\|\mathcal{S}_{q,k} - \mathcal{S}_{q^\dagger,k}\| := \left[\sum_{j\geq 1} \sigma_j^p(\mathcal{S}_{q,k} - \mathcal{S}_{q^\dagger,k})\right]^{1/p}, \quad p \in [1, \infty). \tag{4.1}$$

The (right) singular values are ordered according to

$$\sigma_1(\mathcal{S}_{q,k} - \mathcal{S}_{q^\dagger,k}) \geq \sigma_2(\mathcal{S}_{q,k} - \mathcal{S}_{q^\dagger,k}) \geq \sigma_3(\mathcal{S}_{q,k} - \mathcal{S}_{q^\dagger,k}) \geq \cdots \geq 0,$$

and are obtained as the eigenvalues of $[(\mathcal{S}_{q,k} - \mathcal{S}_{q^\dagger,k})^*(\mathcal{S}_{q,k} - \mathcal{S}_{q^\dagger,k})]^{1/2}$. We note that $p = 2$ coincides with the Hilbert-Schmidt norm and that $p = 1$ coincides with the trace-class norm. The right singular functions associated with $\sigma_j(\mathcal{S}_{q,k} - \mathcal{S}_{q^\dagger,k})$ are denoted by ψ_j. Because

$$\|(\mathcal{S}_{q,k} - \mathcal{S}_{q^\dagger,k})\psi_j\| = \sigma_j(\mathcal{S}_{q,k} - \mathcal{S}_{q^\dagger,k}),$$

we have the alternative representation

$$\|\mathcal{S}_{q,k} - \mathcal{S}_{q^\dagger,k}\| = \left[\sum_{j\geq 1} \|(\mathcal{S}_{q,k} - \mathcal{S}_{q^\dagger,k})\psi_j\|^p \right]^{1/p}. \tag{4.2}$$

For the purpose of iterative optimization, we can threshold this expansion,

$$\|\mathcal{S}_{q,k} - \mathcal{S}_{q^\dagger,k}\| \approx \left[\sum_{j=1}^{N} \|(\mathcal{S}_{q,k} - \mathcal{S}_{q^\dagger,k})\psi_j\|^p \right]^{1/p}.$$

In this case, the right singular functions, $\psi_1, \ldots, \psi_N$, become the natural choice of blending functions.

We have reduced the operator norm to a finite sum of terms with a (common) Hilbert space ($H^{3/2}(\partial\Omega)$) norm. This simplifies the formulation of the Landweber iteration: For given $(\psi_j)_{j=1}^N$, we define the nonlinear Hilbert-space valued operator,

$$F_N:\ q \to (\mathcal{S}_{q,k}(\psi_j))_{j=1}^N.$$

For the sake of completeness we give this iteration in the Appendix. In practice, one takes $p = 2$. In the iteration, one would not re-evaluate the right singular functions at each update. Instead, one would, for example, determine these functions for the initial model and use them as blending functions throughout the iteration.

5. A numerical experiment. We consider $n = 3$. We use a finite-difference approximation to solve the Helmholtz equation, that is, to compute the kernel, $\mathcal{G}_{q,k}$, of $\mathcal{S}_{q,k}$, on $\partial\Omega \times \partial\Omega$ off its diagonal, for $q = q^\dagger$ and q given by a smoothed version of $q^\dagger$, which is representative of an initial model in the iteration. As a model for $q^\dagger$ we use a part of SEAM3D, and we set the frequency to 4 Hz. The size of the model is $201 \times 201 \times 201$ with a stepsize of 20 m. We choose source (y_j) and receiver (x_i) points on a lattice with a spacing of 80 m, which samples $\Sigma \subset \partial\Omega$; $i, j = 1, \ldots, 31$. We flatten the residual "data" matrix in the usual way to obtain a 961×961 matrix.

We show the models for q and $q^\dagger$ in Figure 2. In Figure 3 we illustrate $\mathcal{G}_{q,k}(x_i, y_j) - \mathcal{G}_{q^\dagger,k}(x_i, y_j)$ for $i, j = 1, \ldots, 31$. In Figure 4 we illustrate the singular spectrum of $\mathcal{S}_{q,k} - \mathcal{S}_{q^\dagger,k}$. We confirm the asymptotic rapid decay. We also observe a "knee", which may be used a guide to truncating the spectrum. The constants in the decay estimate naturally depend on frequency.

In Figure 5 we illustrate the right singular vector associated with the largest singular value, and in Figure 6 we show the interior solution of the Hemholtz equation generated by this singular vector as a boundary source. This singular vector is expected to recover the most signicifant component that the acquisition surface (Σ) has resolution for.

Acknowledgment. The authors would like to thank Plamen Stefanov for his invaluable suggestions, and Shen Wang for generating the numerical example. This research was funded in part by the members, BGP, ConocoPhillips, ExxonMobil, PGS, Statoil and Total, of the Geo-Mathematical Imaging Group at Purdue University.

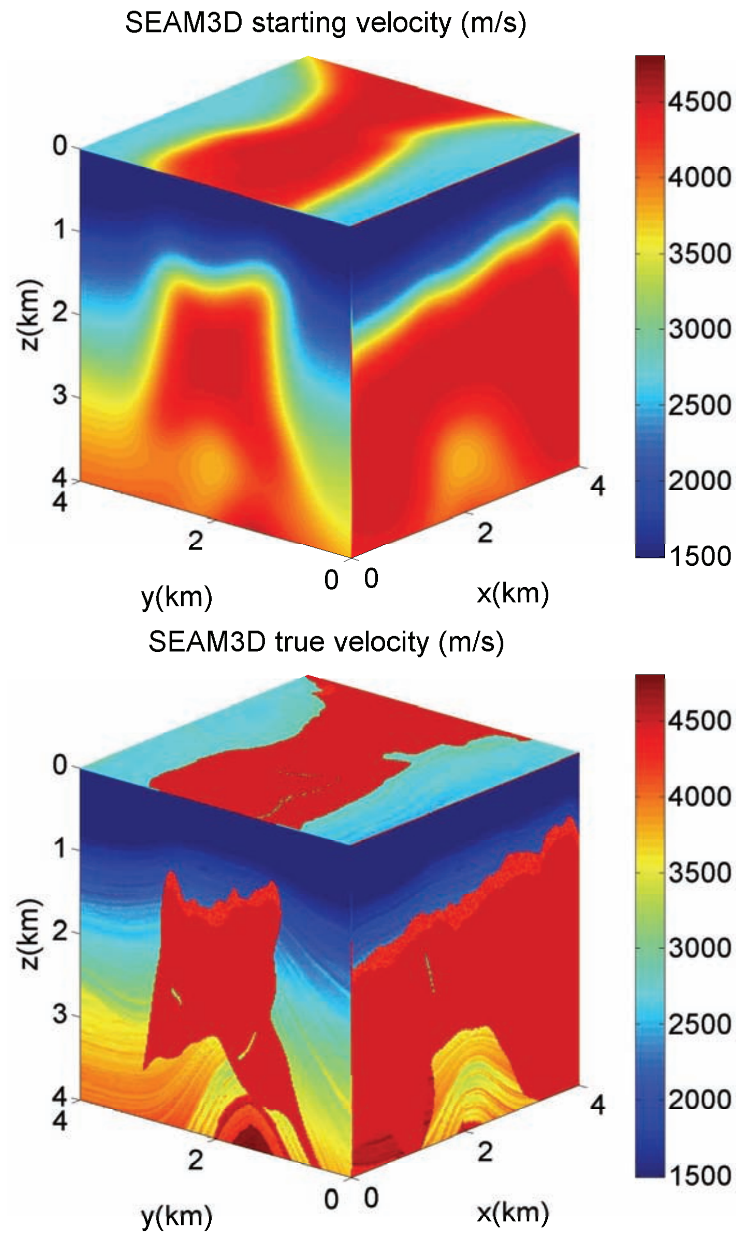

FIG. 2. *Illustrations of c and $c^\dagger$; the models are $\omega^2 c^{-2}$ (top) and $\omega^2 (c^\dagger)^{-2}$ (bottom). We set $\omega/2\pi = 4$ Hz.*

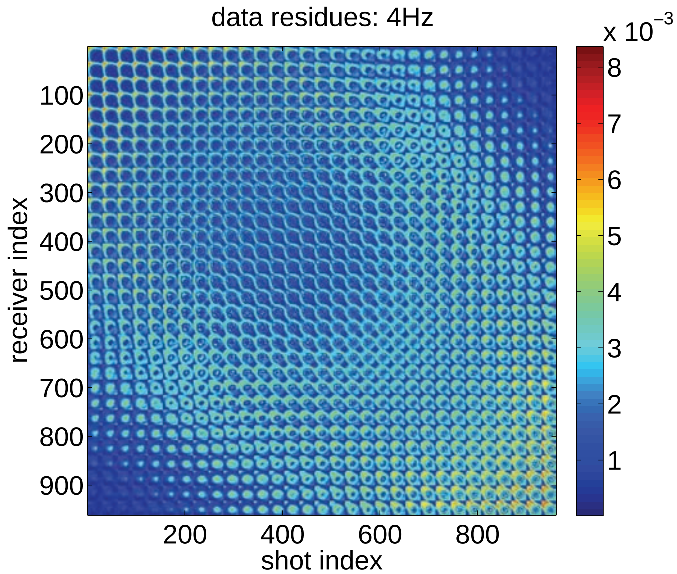

Fig. 3. *The discrete approximation of $\mathcal{G}_{q,k}(x, y) - \mathcal{G}_{q^\dagger,k}(x, y)$; both x and y sample the acquisition plane (Σ) and their coordinate pairs are flattened in an array.*

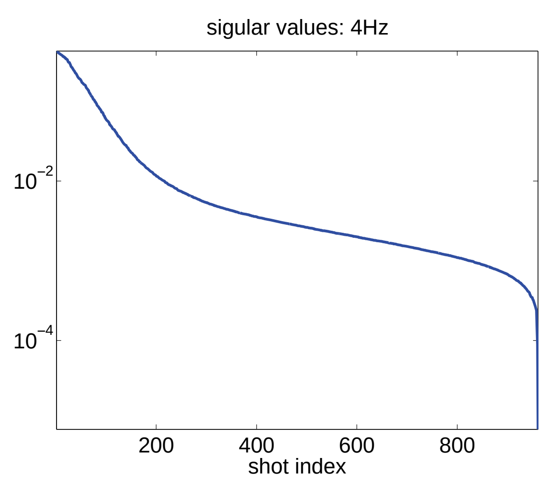

Fig. 4. *The singular spectrum of the discrete approximation of $\mathcal{S}_{q,k} - \mathcal{S}_{q^\dagger,k}$.*

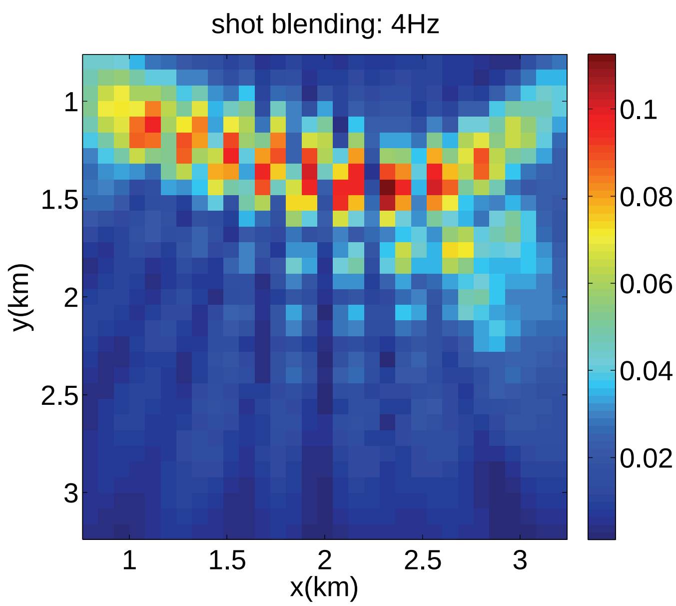

FIG. 5. *The right singular vector associated with the largest value in the singular spectrum.*

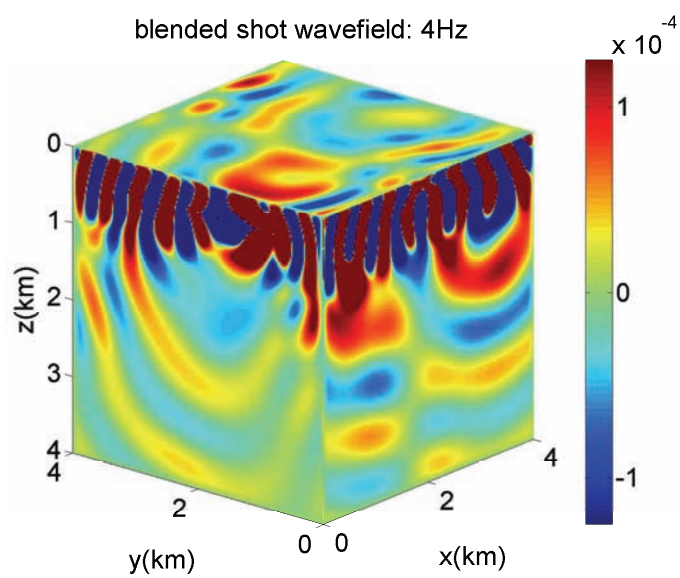

FIG. 6. *The interior solution generetaed by the singular vector illustrated in Figure 5 as a boundary source.*

Appendix A. Nonlinear Landweber iteration with blending.

We consider time-harmonic waves, described by solutions, u say, of the Helmholtz equation on $\mathbb{R}^n$, $n \geq 3$. We write

$$q(x) = -\omega^2 c^{-2}(x)$$

(which is $\tilde{q}(x)$ in the main text by abuse of notation); $\omega \in \mathbb{R}$. We introduce a bounded open (computational) domain $\Theta \subset \mathbb{R}^n$ with boundary in $C^{(1,1)}$. We assume that $\Theta' = \mathbb{R}^n \backslash \overline{\Theta}$ is connected. We consider the problem,

$$\text{(A.1)} \qquad \left\{ \begin{array}{rcll} (-\Delta - \quad k^2)u &=& 0, & x \in \Theta' \quad , \\ (-\Delta + q(x))u &=& f, & x \in \Theta \quad , \\ \lim\limits_{r\to\infty} r^{(n-1)/2} \left(\dfrac{\partial u}{\partial r} - \mathrm{i}ku \right) &=& 0 & \quad . \end{array} \right.$$

Here, $q \in L^\infty(\Theta)$ while $-k^2 = -\omega^2 c_\infty^{-2}$, where c_∞ is constant.

We replace (A.1) by the equivalent problem on Θ,

$$\text{(A.2)} \qquad \left\{ \begin{array}{rcll} (-\Delta + q(x))u &=& f, & x \in \Theta \quad , \\ \dfrac{\partial u}{\partial \nu} &=& -\Lambda_e u, & x \in \partial\Theta \quad , \end{array} \right.$$

where Λ_e is the exterior Dirichlet-to-Neumann map for the Helmholtz equation on Θ'. We introduce an open bounded domain, D, with $D \subset \Theta$ and a boundary in $C^{(1,1)}$, and $D' = \mathbb{R}^n \backslash \overline{D}$ being connected. Let Σ be an open portion of ∂D. In the above, furthermore, f represents volume sources supported in ∂D; this property will be implicit through the introduction of an appropriate Dirac measure and factoring out ψ (defined on ∂D) in f .

The solution, u, of (A.2), in $H^1(\Theta)$, also solves the variational equation

$$\text{(A.3)} \qquad b(q; u, v) = s(v) \quad \text{for all } v \in H^1(\Theta),$$

where

$$\text{(A.4)} \qquad b(q; u, v) = \int_\Theta (\nabla u \cdot \nabla \bar{v} - q\, u\bar{v})\, \mathrm{d}x,$$

and

$$\text{(A.5)} \qquad s(v) = \int_\Theta f\, \bar{v}\, \mathrm{d}x - \int_{\partial\Theta} (\Lambda_e u)\, \bar{v}\, \mathrm{d}\sigma.$$

We consider the one-parameter family of models, q_t, with $q_0 = q$, and a set of source functions, $(f_k(x))_{k=1}^N$; we collect $(u_{k,t}(x))_{k=1}^N$ satisfying

$$\text{(A.6)} \qquad b(q_t; u_{k,t}, v) = s_k(v) \quad \text{for all } v \in H^1(\Theta),$$

with

$$\text{(A.7)} \qquad s_k(v) = \int_\Theta f_k\, \bar{v}\, \mathrm{d}x - \int_{\partial\Theta} (\Lambda_e u)\, \bar{v}\, \mathrm{d}\sigma.$$

(The first integral on the right-hand side is effectively an integral over ∂D.) We write the solution, $u_{k,t}$, restricted to ∂D as an operator, $\mathcal{S}(q_t)$ (which can be identified with $\mathcal{S}_{q_t - k^2, k}$), acting on f_k, and introduce the functional,

$$\text{(A.8)} \qquad \mathcal{J}(q_t) = \frac{1}{2} \sum_{k=1}^N \|\mathcal{P}\left(\mathcal{S}(q_t) f_k - d_{f,k}\right)\|^2_{L^2(\partial D)};$$

here, $(d_{f,k}(x))_{k=1}^N$ represents the data, and $\mathcal{P}$ is an elliptic operator such that $\|\mathcal{P}\, d\|_{L^2(\partial D)} = \|d\|_{H^{3/2}(\partial D)}$.

Taking the derivative with respect to t yields

$$\frac{\mathrm{d}}{\mathrm{d}t}\mathcal{J}(q_t)\bigg|_{t=0} = \sum_{k=1}^N \mathrm{Re}\int_\Sigma [\mathcal{P}^*\mathcal{P}(\mathcal{S}(q_t)f_k - d_{f,k})]\ \frac{\mathrm{d}}{\mathrm{d}t}\mathcal{S}(q_t)f_k\bigg|_{t=0}\mathrm{d}\sigma. \tag{A.9}$$

We introduce $v = (v_k(x))_{k=1}^N$, Lagrange multipliers $(w_k(x))_{k=1}^N$ and a family of functionals,

$$\mathcal{L}(q_t; v, w) = \mathcal{J}(q_t) + \sum_{k=1}^N \mathrm{Re}\ (b(q_t; v_k, w_k) - s_k(w_k)), \tag{A.10}$$

where $\mathcal{S}(q_t)f_k$ in $\mathcal{J}(q_t)$ is replaced by v_k. If $v_k = u_{k,t}$ is the solution of the direct problem (A.6),

$$\mathcal{L}(q_t; u_t, w) = \mathcal{J}(q_t) \quad \text{for all } w_k \in H^1(\Theta),\ k = 1, \ldots, N,$$

then

$$\begin{aligned}\frac{\mathrm{d}}{\mathrm{d}t}\mathcal{L}(q_t; u_t, w)\bigg|_{t=0} = \sum_{k=1}^N \mathrm{Re}\ \Bigg\{ \Bigg[\int_\Sigma [\mathcal{P}^*\mathcal{P}(\mathcal{S}(q_t)f_k - d_{f,k})]\ \frac{\mathrm{d}}{\mathrm{d}t}\mathcal{S}(q_t)f_k\bigg|_{t=0}\mathrm{d}\sigma \\ + b\left(q; \frac{\mathrm{d}}{\mathrm{d}t}\mathcal{S}(q_t)f_k\bigg|_{t=0}, w_k\right)\Bigg] + \frac{\mathrm{d}}{\mathrm{d}t}b(q_t; u_k, w_k)\bigg|_{t=0}\Bigg\}\end{aligned}$$

for all $w_k \in H^1(\Theta)$. If w_k solves

$$b(q; v, w_k) = -\int_\Sigma [\mathcal{P}^*\mathcal{P}(\mathcal{S}(q_t)f_k - d_{f,k})]\ v\,\mathrm{d}\sigma \quad \text{for all } v \in H^1(\Theta),\ k = 1, \ldots, N, \tag{A.11}$$

then

$$\frac{\mathrm{d}}{\mathrm{d}t}\mathcal{L}(q_t, u_t, w)\bigg|_{t=0} = \sum_{k=1}^N \mathrm{Re}\ \frac{\mathrm{d}}{\mathrm{d}t}b(q_t; u_k, w_k)\bigg|_{t=0}. \tag{A.12}$$

We can write (A.11) in the form of the direct problems:

$$b(q; \bar{w}_k, v) = -\int_\Sigma [\mathcal{P}^*\mathcal{P}(\mathcal{S}(q_t)f_k - d_{f,k})]\ \bar{v}\,\mathrm{d}\sigma \quad \text{for all } v \in H^1(\Theta),\ k = 1, \ldots, N; \tag{A.13}$$

here, $(\bar{w}_k)_{k=1}^N$ is the so-called adjoint state, with $\bar{w}_k \in H^1(\Theta)$ being the solution to

$$\left\{\begin{array}{rcll} (-\Delta - \quad k^2)\bar{w}_k &=& 0, \quad x \in \Theta' &, \\ (-\Delta + q(x))\bar{w}_k &=& [\mathcal{P}^*\mathcal{P}(\mathcal{S}(q_t)f_k - d_{f,k})]\,\delta_\Sigma, \quad x \in \Theta &, \\ \lim\limits_{r\to\infty} r^{(n-1)/2}\left(\dfrac{\partial \bar{w}_k}{\partial r} - \mathrm{i}k\bar{w}_k\right) &=& 0 &. \end{array}\right. \tag{A.14}$$

Again, we have the equivalent problems

$$\left\{\begin{array}{rcll} (-\Delta + q(x))\bar{w}_k &=& [\mathcal{P}^*\mathcal{P}(\mathcal{S}(q_t)f_k - d_{f,k})]\,\delta_\Sigma, \quad x \in \Theta &, \\ \dfrac{\partial \bar{w}_k}{\partial \nu} &=& -\Lambda_e\bar{w}_k, \quad x \in \partial\Theta &. \end{array}\right. \tag{A.15}$$

We have made use of the fact that $\Lambda_e^*(\bar{w}_k) = \overline{\Lambda_e w_k}$. We then evaluate

$$\frac{\mathrm{d}}{\mathrm{d}t}b(q_t; u_k, w_k)\bigg|_{t=0} = -\int_\Theta u_k\bar{w}_k\,\frac{\mathrm{d}}{\mathrm{d}t}q_t\bigg|_{t=0}\mathrm{d}x. \tag{A.16}$$

We identify

$$\frac{\mathrm{d}}{\mathrm{d}t} q_t \bigg|_{t=0} \quad \text{with} \quad \gamma.$$

Thus

$$d\mathcal{J}(q,\gamma) = -\sum_{k=1}^{N} \mathrm{Re} \int_{\Theta} u_k \bar{w}_k \, \gamma \, \mathrm{d}x =: (\rho,\gamma)_{L^2(\Theta)}. \tag{A.17}$$

The gradient flow can be chosen to optimize the functional. In general, we can introduce a duality pairing, $\mathcal{V}', \mathcal{V}$, defined by $\langle .,. \rangle$, a bilinear (continuous and coercive) form. We then let $\gamma \in \mathcal{V}'$ be the solution to

$$\langle \gamma, \tilde{\gamma} \rangle = -(\rho, \tilde{\gamma})_{L^2(\Theta)} \quad \text{for all } \tilde{\gamma} \in \mathcal{V}.$$

If $\mathcal{B}$ is an elliptic operator such that $(\mathcal{B}\gamma, \tilde{\gamma})_{L^2(\Theta)} = \langle \gamma, \tilde{\gamma} \rangle$, then the gradient flow is called a $\mathcal{B}$-gradient flow.

We shift this equation in t from 0 to discrete values, t_n:

$$\langle \gamma_n, \tilde{\gamma} \rangle = -(\rho_n, \tilde{\gamma})_{L^2(\Theta)} \quad \text{for all } \tilde{\gamma} \in \mathcal{V}$$

and use a forward Euler scheme to get

$$q_{n+1} = q_n + \tau \gamma_n,$$

which represents the nonlinear Landweber iteration with stepsize τ.

REFERENCES

[1] G. Alessandrini and S. Vessela, *Lipschitz stability for the inverse conductivity problem*, Adv. in Appl. Math., 35 (2005), pp. 207–241.

[2] C.J. Beasley, R.E. Chambers, and Z. Jiang, *A new look at simultaneous sources*, in Expanded Abstracts, Society of Exploration Geophysicists, 1998, pp. 133–135.

[3] E. Beretta, M.V. De Hoop, and L. Qiu, *Lipschitz stability of an inverse boundary value problem for a schrödinger equation*, p. submitted.

[4] A.J. Berkhout, *Seismic procesing in the inverse data space*, Geophysics, 71 (2006), pp. A29–A33.

[5] A.J. Berkhout, *Changing the mindset in seismic data acquisition*, The Leading Edge, 27 (2008), pp. 924–938.

[6] A.J. Berkhout, G. Blacquire, and E. Verschuur, *From simultaneous shooting to blended acquisition*, in Expanded Abstracts, vol. 27, Society of Exploration Geophysicists, 2008, pp. 2831–2838.

[7] L. Borcea, G.A. Gray, and Y. Zhang, *Variationally constrained numerical solution of electrical impedance tomography*, Inverse Problems, 19 (2003), pp. 1159–1184.

[8] Y. Capdeville, Y. Gung, and B. Romanowicz, *Towards global earth tomography using the spectral element method: A technique based on source stacking*, Geophys. J. Int., 162 (2005), pp. 541–554.

[9] M. Choulli and P. Stefanov, *Stability for the multi-dimensional borg-levinson theorem with partial boundary data*, p. submitted.

[10] D. Colton and R. Kress, *Inverse acoustic and electromagnetic scattering theory*, vol. 93 of Applied Mathematical Sciences, Springer, Berlin, 1992.

[11] W. Dai and G.T. Schuster, *Least-squares migration of simultaneous sources data with a deblurring filter*, in Expanded Abstracts, Society of Exploration Geophysicists, 2009, pp. 2990–2994.

[12] M.V. De Hoop, L. Qiu, and O. Scherzer, *Local analysis of inverse problems: Hölder stability and iterative reconstruction*, Inverse Problems, (2012), p. in print.

[13] F. Gao, A. Atle, and P. Williamson, *Full waveform inversion using deterministic source encoding*, in Expanded Abstracts, vol. 29, Society of Exploration Geophysicists, 2010, pp. 1013–1017.

[14] D. Gilbarg and N.S. Trudinger, *Elliptic partial differential equations of second order*, vol. 224 of Grundlehren der Mathematischen Wissenschaften [Fundamental Principles of Mathematical Sciences], Springer-Verlag, Berlin, second ed., 1983.

[15] D.G. Gisser, D. Isaacson, and J.C. Newell, *Electric current computational tomography and eigenvalues*, SIAM Journal on Applied Mathematics, 50 (1990), pp. 1623–1634.

[16] V. Isakov, *Inverse problems for partial differential equations*, vol. 127 of Applied Mathematical Sciences, Springer, New York, second ed., 2006.

[17] J. Krebs, J. Anderson, D. Hinkley, R. Neelamani, S. Lee, A. Baustein, and M.-D. Lacasse, *Fast full-wavefield seismic inversion using encoded sources*, Geophysics, 74 (2009), pp. WCC177–WCC188.

[18] A.I. Nachman, *Reconstruction from boundary measurements*, Ann. of Math. (2), 128 (1988), pp. 531–576.

[19] A.I. Nachman, J. Sylvester, and G. Uhlmann, *An n-dimensional borg-levinson theorem*, Communications in Mathematical Physics, 115 (1988), pp. 595–605.

[20] R. Neelamani, C. Krohn, J. Krebs, J. Romberg, M. Deffenbaugh, and J. Anderson, *Efficient seismic forward modelling using simultaneous random sources and sparsity*, Geophysics, 75 (2010), pp. WB15–WB27.

[21] W.E.A. Rietveld and A.J. Berkhout, *Prestack depth migration by means of controlled illumination*, Geophysics, 59 (1994), pp. 801–809.

[22] J. Stefani, G. Hampson, and E.F. Herkenhoff, *Acquisition using simultaneous sources*, in Extended Abstracts, European Association of Geoscientists and Engineers, 2007, p. B006.

[23] D. Vigh and W. Starr, *3d prestack plane-wave, full-waveform inversion*, Geophysics, 73 (2008), pp. VE135–VE144.

[24] S. Wang, M.V. De Hoop, and J. Xia, *On 3d modeling of seismic wave propagation via a structured massively parallel multifrontal direct helmholtz solver*, Geophys. Prosp., 59 (2011), pp. 857–873.

[25] N.D. Whitmore, *An imaging hierarchy for common angle plane wave seismograms*, PhD thesis, University of Tulsa, 1995.